Fish & Shellfish Immunology 49 (2016) 450–460

Contents lists available at ScienceDirect

Fish & Shellfish Immunology

journal homepage: www.elsevier.com/locate/fsi

Full length article

First comparative characterization of three distinct ferritin subunits from a teleost: Evidence for immune-responsive mRNA expression and iron depriving activity of seahorse (*Hippocampus abdominalis*) ferritins

Minyoung Oh [a, b], Navaneethaiyer Umasuthan [a, b], Don Anushka Sandaruwan Elvitigala [a, b], Qiang Wan [a, b], Eunyoung Jo [a, b], Jiyeon Ko [a, b], Gyeong Eon Noh [c], Sangok Shin [c], Sum Rho [c], Jehee Lee [a, b, *]

[a] Department of Marine Life Sciences, School of Marine Biomedical Sciences, Jeju National University, Jeju Self-Governing Province 63243, Republic of Korea
[b] Fish Vaccine Development Center, Jeju National University, Jeju Self-Governing Province 63243, Republic of Korea
[c] Corea Cheju Origin Roh's Aquariums, Jongdal-ri, Gujwa-eup, Jeju Self-Governing Province 63364, Republic of Korea

ARTICLE INFO

Article history:
Received 5 August 2015
Received in revised form
21 December 2015
Accepted 28 December 2015
Available online 31 December 2015

Keywords:
Big belly seahorse
Ferritin H, L, and M subunits
Tissue mRNA expression
Immune response
Iron (II) chelation/withholding

ABSTRACT

Ferritins play an indispensable role in iron homeostasis through their iron-withholding function in living beings. In the current study, cDNA sequences of three distinct ferritin subunits, including a ferritin H, a ferritin M, and a ferritin L, were identified from big belly seahorse, *Hippocampus abdominalis*, and molecularly characterized. Complete coding sequences (CDS) of seahorse ferritin H (*HaFerH*), ferritin M (*HaFerM*), and ferritin L (*HaFerL*) subunits were comprised of 531, 528, and 522 base pairs (bp), respectively, which encode polypeptides of 177, 176, and 174 amino acids, respectively, with molecular masses of ~20–21 kDa. Our *in silico* analyses demonstrate that these three ferritin subunits exhibit the typical characteristics of ferritin superfamily members including iron regulatory elements, domain signatures, and reactive centers. The coding sequences of *HaFerH, M*, and *L* were cloned and the corresponding proteins were overexpressed in a bacterial system. Recombinantly expressed HaFer proteins demonstrated detectable *in vivo* iron sequestrating (ferroxidase) activity, consistent with their putative iron binding capability. Quantification of the basal expression of these three *HaFer* sequences in selected tissues demonstrated a gene-specific ubiquitous spatial distribution pattern, with abundance of mRNA in *HaFerM* in the liver and predominant expression of *HaFerH* and *HaFerL* in blood. Interestingly, the basal expression of all three ferritin genes was found to be significantly modulated against pathogenic stress mounted by lipopolysaccharides (LPS), poly I:C, *Streptococcus iniae*, and *Edwardsiella tarda*. Collectively, our findings suggest that the three HaFer subunits may be involved in iron (II) homeostasis in big belly seahorse and that they are important in its host defense mechanisms.

1. Introduction

Ferritin is an important protein that primarily regulates the cellular concentration of free iron (II) in living organisms. It can serve as a potent iron depriver and thereby plays a crucial role in the storage and detoxification of iron [1,2]. Ferritin is comprised of 24 subunits, which form a hollow shell that can mineralize about 4500 iron atoms in it. In vertebrates, the 24-mer globular protein of ferritin is made up of heavy (H) and light (L) subunits, which are encoded by two distinct genes. The H subunit harbors the ferroxidase center that converts ferrous ions (Fe^{2+}) into ferric ions (Fe^{3+}) [3], whereas the L subunit contains a site for nucleation with a mineral core to facilitate iron nucleation [4]. In mammals, the differential proportion of H and L subunits in ferritin is clearly tissue-dependent: heart ferritin is enriched with H subunits, whereas liver ferritin predominantly contains L subunits. Although similar architectural characteristics are found among ferritins from

* Corresponding author. Marine Molecular Genetics Lab, Department of Marine Life Sciences, College of Ocean Science, Jeju National University, 66 Jejudaehakno, Ara-Dong, Jeju 690-756, Republic of Korea.
E-mail address: jehee@jejunu.ac.kr (J. Lee).

http://dx.doi.org/10.1016/j.fsi.2015.12.039
1050-4648/

different animal origins, these subunits largely vary at the amino acid level, which permits them to play different roles in iron homeostasis [1]. Interestingly, a third subunit known as the middle (M) type subunit has also been identified besides the aforementioned two subunits, almost exclusively from the lower vertebrates [5,6]. The M subunit was found to possess both the ferroxidase center of the H subunit and the iron nucleation site of the L subunit, and it thus exhibits the functional properties of both H and L subunits [7].

The expression of ferritin subunits is a tightly regulated process that is controlled at transcriptional as well as post-transcriptional levels [7]. These three ferritin subunits harbor a regulatory sequence known as the iron responsive element (IRE) in their 5′-untranslated region (UTR), which is important in sensing heavy iron loads and which in turn modulates subunit expression [8] with the aid of iron regulatory proteins (IRPs) [7]. Moreover, a wide array of factors modulate the basal expression level of ferritin genes. In addition to iron load [9], ferritin transcription was found to be modulated by oxidative stress [10], temperature [11], heavy metals [12], hormones, and cytokines [7]. Moreover, the regulated expression of ferritin genes upon administering pathogen-associated molecular patterns (PAMPs) and/or pathogenic infections has also been reported [10,13]. Consequently, ferritin has been proposed to be an acute phase protein that is involved in innate immune responses against invading pathogens mainly through its iron withholding function [14,15].

Ferritin is ubiquitously distributed throughout the biota from microbes to humans, and ferritin genes encoding distinct subunits have been identified in a diverse group of invertebrate and vertebrate species, including fish. For instance, the *ferritin H* gene has been reported from *Ictalurus punctatus* [16], *Scophthalmus maximus* [17], *Dicentrarchus labrax* [13], *Salmo salar* [5,18], and *Oplegnathus fasciatus* [19]. Meanwhile, the *ferritin M* gene has been characterized from several marine teleost species, including *Cynoglossus semilaevis* [20], *Pseudosciaena crocea* [21], *Sciaenops ocellatus* [22], *S. maximus* [10], *S. salar* [5], and *O. fasciatus* [6]. However, the *ferritin L* gene has not yet been cloned from any fish species. Ferritin has been studied in terms of its iron chelating activity, DNA protection effect, bacteriostatic function, and transcriptional regulation abilities under different stress conditions. However, comprehensive and comparative studies that describe all the ferritin subunits from a single species are very limited [23].

The big belly seahorse (*Hippocampus abdominalis*) is an important resource in oriental medicine as practiced in China, Korea, and Japan. However, this species has been listed under the CITES (Convention on International Trade in Endangered Species of Wild Fauna and Flora). Moreover, seahorses are vulnerable to pathogenic attacks leading to fatal diseases [24,25]. Therefore, it is important to explore the immune mechanisms existing in seahorses to gain an insight into their immune system at the molecular level.

In this study, we have identified and functionally characterized homologs of the ferritin H, ferritin M, and ferritin L subunits from seahorse, designated respectively as *HaFerH*, *HaFerM*, and *HaFerL*. In addition, the basal as well as the temporally modulated expression levels of each *HaFer* gene following PAMP or pathogen treatment were detected. Finally, the iron depriving activity of these ferritin subunits was demonstrated using recombinant proteins.

2. Materials and methods

2.1. Construction of seahorse cDNA database

The database of seahorse cDNA sequences was constructed by the 454 GSFLX™ sequencing technique. Briefly, total RNA was extracted from blood, liver, kidney, gill, and spleen tissues of 18 seahorses. The extracted RNA was then cleaned with an RNeasy Mini kit (Qiagen, USA) and assessed for quality and quantified using an Agilent 2100 Bioanalyzer (Agilent Technologies, Canada), which detected an RNA integration score (RIN) of 7.1. For GS-FLX 454 shotgun library preparation, the RNA was fragmented into an average size of 1147 bp using the Titanium system (Roche 454 Life Science, USA). Sequencing was finally run on half a picotiter plate on a Roche 454 GS-FLX^{TM} DNA platform at Macrogen, Korea. The raw 454 reads were trimmed to remove adapter and low-quality sequences, and de novo assembled into contigs using GS Assembler (Roche 454 Life Science, USA) with the default parameters. The Nile tilapia genome obtained from NCBI GenBank was used as a reference genome for mapping analysis.

2.2. Identification of sequences of three different ferritin subunits from sea horse cDNA database

The cDNA sequences of *HaFerH* (Accession number: KP780174), *HaFerM* (Accession number: KP780175), and *HaFerL* (Accession number: KP780176), which showed prominent similarity with the known ferritin subunits of other vertebrates, were identified from the above established cDNA database using the Basic Local Alignment Tool (BLAST) (http://blast.ncbi.nlm.nih.gov/Blast.cgi) available at the National Center for Biotechnology Information (NCBI). In order to obtain the full sequence of the 5′-UTR, 5′ rapid amplification of cDNA ends (RACE) was performed with a FirstChoice® RLM-RACE kit using gene-specific oligomers (Table 1).

2.3. Sequence characterization and phylogenetic analysis

Three identified HaFer sequences were characterized using several *in silico* tools. The putative complete open reading frames (ORFs) of *HaFer* sequences were determined and the corresponding amino acid sequences were deduced using DNAsist 2.2 software. The IRE in the 5′-UTR was predicted using SIREs Web Server 2.0 (http://ccbg.imppc.org/sires/). The protein domains of derived amino acid sequences were predicted using the ExPASy Prosite database (http://prosite.expasy.org). Physicochemical properties of HaFer sequences were determined using the ProtParam tool (http://web.expasy.org/protparam). Pairwise and multiple sequence comparisons of HaFer sequences with their respective homologs were performed using the EMBOSS needle (http://www.Ebi.ac.uk/Tools/emboss/align) and ClustalW2 (http://www.Ebi.ac.uk/Tools/clustalw2) programs, respectively. A phylogenetic reconstruction of HaFer sequences and their orthologs was generated by employing the neighbor-joining (NJ) method in Molecular Evolutionary Genetics Analysis version 4.0 (MEGA 4.0) software [26].

2.4. Cloning the ORFs of HaFer genes

The ORFs of *HaFerH*, *HaFerM*, and *HaFerL* were PCR amplified with corresponding cloning primers appended with *Eco*RI and *Hind*III restriction sites (Table 1) using the seahorse liver cDNA as a template and cloned into the pMAL-c2X vector. Briefly, PCR was performed in a 50 μL reaction mixture containing 4 units (U) of Ex Taq polymerase, 5 μL of 10 × Ex Taq buffer, 4 μL of 2.5 mM dNTPs, 25 pmol of each primer, and 50 ng of liver cDNA. The PCR was performed as follows: initial denaturation at 94 °C for 3 min, followed by 30 cycles of 94 °C for 30 s, 55 °C for 30 s, 72 °C for 40 s, and a final extension step at 72 °C for 4 min. The PCR product was gel-purified using an Accuprep™ gel purification kit (Bioneer, Korea). The PCR product and pMAL-c2X vector were then digested with restriction enzymes and gel-purified again. Finally, the digested pMAL-c2X vector and PCR product were ligated using Mighty Mix (5.0 μl; TaKaRa, Japan) at 4 °C overnight. The ligated pMAL-c2X/

Table 1
Sequences of the primers used in the study.

Purpose	Orientation	Primer sequences
40S ribosomal protein S7 qPCR	Forward	GCGGGAAGCATGTGGTCTTCATT
40S ribosomal protein S7 qPCR	Reverse	ACTCCTGGGTCGCTTCTGCTTATT
Ferritin H qRT-PCR	Forward	ACTGCGAGGCTGCAATCAACA
Ferritin H qRT-PCR	Reverse	CCTGGTCATCCCGGTCAAAGTAGTAA
Ferritin M qRT-PCR	Forward	CAAGAAACCAGAGCGTGATGAGTGG
Ferritin M qRT-PCR	Reverse	GTCCACATGCTCAGAGGCCAATTT
Ferritin L qRT-PCR	Forward	GGACGACGTTGCCCTGAAGAAAT
Ferritin L qRT-PCR	Reverse	CCCGCGTTGGTTTAGCGATAGT
Ferritin H cloning	Forward	GAGAGAgaattcATGAGTTCCCAGGTGAGACAAAACTTC
Ferritin H cloning	Reverse	GAGAGAaagcttTTAACTGCTTTCCTTGCCCAAAGTATGT
Ferritin M cloning	Forward	GAGAGAgaattcATGGAGTCTCAAGTGCGCCAGA
Ferritin M cloning	Reverse	GAGAGAaagcttTTAGCTCTTGCCCTCCAGAGAGT
Ferritin L cloning	Forward	GAGAGAgaattcATGCAGTCGGTGGTCCG
Ferritin L cloning	Reverse	GAGAGAaagcttTTACAAAGTGTGCTTGTCAAAGAGGTATTC
Ferritin H 5′ RACE Outer	Reverse	GGCTTCCTGACATCTTGAAGGAAGATCCT
Ferritin H 5′ RACE Inner	Reverse	TCTTCGTGAGATTGGTCCCGGAAGAA
Ferritin M 5′ RACE Outer	Reverse	TGTTCCCTTTCCTCCTCGCTGTTCT
Ferritin M 5′ RACE Inner	Reverse	CGGTTAATGGCGGCCTCGCAT
Ferritin L 5′ RACE Outer	Reverse	GTGTTCTTGTTCCTTTTGAGAGAGCGCCA
Ferritin L 5′ RACE Middle	Reverse	ACTGGAAAATTTCTTCAGGGCAACGTCGT
Ferritin L 5′ RACE Inner	Reverse	TCGCCTTCACACTCGGCGT
5′ RACE Outer Primer	Forward	GCTGATGGCGATGAATGAACACTG
5′ RACE Inner Primer	Forward	CGCGGATCCGAACACTGCGTTTGCTGGCTTTGATG

HaFer product was then transformed into *Escherichia coli* DH5α cells and sequenced.

2.5. Over-expression and purification of recombinant HaFer fusion proteins

The sequence confirmed recombinant constructs (pMAL-c2X/HaFerH, pMAL-c2X/HaFerM, and pMAL-c2X/HaFerL) were transformed into competent *E. coli* BL21 (DE3) cells. Transformed colonies were grown in 500 mL LB broth containing 100 μg/mL ampicillin and 1% glucose with shaking at 37 °C. After the optical density at 600 nm reached 0.5, isopropyl-β-thiogalactopyranoside (IPTG) was added at a final concentration of 1 mM. The bacterial culture was incubated for 3 h at 37 °C. Subsequently, cells were harvested by centrifugation (3000 rpm for 30 min at 4 °C). The pellet was resuspended in column buffer (20 mM Tris–HCl pH 7.4 and 200 mM NaCl) and stored at −20 °C overnight. On the following day, the bacterial suspension was lysed by cold sonication and centrifuged (13,000 rpm for 20 min at 4 °C) to obtain the supernatant (crude extract). Thereafter, this crude extract was subjected to a purification process using the pMAL™ Protein Fusion and Purification System (New England BioLabs, USA), following the vendor's protocol. The concentration of the eluted purified recombinant proteins was determined by the Bradford method using bovine serum albumin as the standard [27] and the purity was evaluated on a 12% SDS-PAGE under reducing conditions.

2.6. Iron (II) chelating activity assay

In order to determine the potential iron chelating activity of the three HaFer subunits, an iron (II) chelation assay was conducted using purified recombinant proteins as previously described with minor modifications [28]. Briefly, 20 μL of 2 mM $FeSO_4$ was added to 1 mL of recombinant HaFer protein (rHaFer) diluted into different concentrations in a column buffer. Samples were incubated at room temperature (25 °C) for 10 min. Subsequently, 20 μL of 5 mM ferrozine (Sigma, USA) was added to each sample. The contents were mixed thoroughly and then incubated again at room temperature for 15 min. Finally, the optical density (OD) of each sample was measured at 562 nm using a spectrophotometer (Thermo Scientific, USA).

2.7. Experimental animals and tissue collection

Seahorses were purchased from the Korea Marine Ornamental Fish Breeding Center in Jeju Island, Republic of Korea. Fish were acclimated in laboratory aquarium tanks (300 L) for one week prior to the experimentation. The sand-filtered seawater was aerated continuously and a constant temperature (18 ± 2 °C) and salinity (34 ± 0.6‰) were maintained throughout the experiment. No food was provided during the challenge experiment. For tissue distribution analysis, six seahorses (3 males and 3 females) with an average body weight of 8 g were used. Blood was collected by tail cutting, and the peripheral blood cells (PBCs) were separated by immediate centrifugation at 3000 *g* for 10 min at 4 °C. Other tissues, including heart, gill, liver, spleen, kidney, intestine, stomach, skin, muscle, pouch, and brain were excised and immediately snap-frozen in liquid nitrogen and stored at −80 °C.

For the immune challenge, seahorses with an average body weight of 3 g were used. LPS (1.25 μg/μL), poly I:C (1.5 μg/μL), *Edwardsiella tarda* (5×10^3 CFU/μL), and *Streptococcus iniae* (10^5 CFU/μL) were prepared with PBS and injected intraperitoneally in a total volume of 100 μL. The fish in the control group were injected with 100 μL PBS. The kidney and liver were sampled from five individuals at 0, 3, 6, 12, 24, 48, and 72 h post-injection (p.i.) as described above.

2.8. Total RNA extraction and cDNA synthesis

Total RNA was extracted from a pool of tissue samples collected from six healthy fish and five immune-challenged fish corresponding to each time point by RNAiso plus (TaKaRa, Japan), followed by clean-up with an RNeasy spin column (Qiagen, USA). RNA quality was examined using 1.5% agarose gel electrophoresis and the concentration was determined at 260 nm in a μDrop Plate (Thermo Scientific, USA). First-strand cDNA was synthesized in a 20 μL reaction mixture containing 2.5 μg of RNA by using the PrimeScript™ II 1st strand cDNA Synthesis Kit (TaKaRa, Japan). The synthesized cDNA was diluted 40-fold in nuclease-free water and stored in a freezer at −80 °C until further use.

2.9. Analysis of mRNA by quantitative real time PCR (qPCR)

To quantify the mRNA expression in different tissues of healthy and immune-challenged animals, qPCR was carried out using a Thermal Cycler Dice™ TP800 (TaKaRa, Japan) in a 10 μL reaction volume containing 3 μL of diluted cDNA template, 5 μL of 2 × TaKaRa Ex Taq™ SYBR premix, 0.5 μL of each of the forward and reverse primers (10 pmol/μL; Table 1), and 1 μL of nuclease free ddH_2O. The qPCR cycle profile included one cycle of 95 °C for 10 s, followed by 35 cycles of 95 °C for 5 s, 58 °C for 10 s, and 72 °C for 20 s, and a final single cycle of 95 °C for 15 s, 60 °C for 30 s, and 95 °C for 15 s. Each assay was conducted in triplicate to increase its credibility. The $2^{-\Delta\Delta Ct}$ method was used to calculate relative expression [29]. Seahorse 40S ribosomal protein S7 (Accession number: KP780177) was used as the internal control gene. Relative mRNA expression in tissues of immune-challenged animals was further normalized to the expression levels of corresponding PBS-injected controls at each time point.

3. Results and discussion

3.1. Molecular characterization of ferritin subunits from H. abdominalis

Significant research has recently been published on teleost ferritins describing the homologs of the H and M subunits [21,30,31]. The existence of multiple isoforms of these subunits has also been demonstrated in fish: (1) three isoforms of *FerH* were identified in rainbow trout [32], and (2) five ferritin isoforms including two *FerH* and three *FerM* were recently cloned from Atlantic salmon [18]. The occurrence of three distinct ferritin subunits in amphibians (tadpole) was evidenced from their differential mRNA expression and electrophoretic features [23]. However, to our best of knowledge, no study has reported all three ferritin subunits from a teleost species. In our study, we isolated the three ferritin subunits H, M, and L from big belly seahorse, *H. abdominalis*, examined their expressional profiles, and assayed their ferroxidase activity.

A search of the *H. abdominalis* cDNA library yielded three partial sequences of ferritin subunits H, M, and L, which we termed *HaFerH*, *HaFerM*, and *HaFerL*, respectively. Molecular profiles of these HaFers are summarized in Table 2. The 5′ RACE was performed to derive the corresponding complete UTRs of *HaFer* cDNAs, and *HaFerH* and *HaFerM* were found to possess the IRE sequences TTACCTGCTTCAACAGTGCTTGAACGGCAAC and GTTCTTGCTTCAACAGTGATTGAACGGAACT, respectively. Alignment of IREs from different vertebrate ferritin subunits revealed considerable conservation, with the FerH homologs in zebrafish and seahorse sharing 100% identity (Fig. 1A). These IREs contained a typical 5′-CAGUGN-3′ loop and a bulged Cys (C8) positioned 6 bp upstream of the loop showing the potential to form a stem-loop structure (Fig. 1B). The IRE in the 5′-UTR is an important element and an acknowledged characteristic of *Fer* genes that modulates their translational regulation [33]. These features suggest that HaFerH and HaFerM expression may also be regulated by iron at the translation level, aided by IRPs.

HaFerH cDNA possessed an ORF of 534 bp coding for 177 amino acids (aa) with a deduced molecular mass of 21 kDa. It contained a 5′-UTR of 607 bp and a 3′-UTR of 479 bp. *HaFerM* cDNA contained a 5′-UTR of 92 bp, an ORF of 531 bp encoding a protein of 176 aa with a predicted molecular mass of 21 kDa, and a 3′-UTR of 35 bp. *HaFerL* transcript contained 5′- and 3′-UTRs of 91 bp and 223 bp, respectively, with a 525 bp ORF translating to a protein of 174 aa (20 kDa). *HaFerH* and *HaFerM* cDNAs also contained a polyadenylation signal (AATAAA) followed by a poly A tail (Table 2).

Analyses of translated amino acid sequences revealed the presence of a ferritin-like diiron domain profile in all three HaFers (residues 7–156). As predicted by the PROSITE tool, HaFerH had two iron-binding region signatures (IBRS1, residues 58–76; IBRS2, residues 123–143), whereas both HaFerM and HaFerL possessed only IBRS2 (residues 123–143) (Fig. 1C). Using the NCBI CDD server, the iron binding sites in the ferroxidase diiron center of HaFerH and HaFerM were found to harbor identical residues (E24, Y31, E58, E59, H62, E104, Q138), but HaFerL exhibited substitutions in a few positions (K24, S31, K58, E59, H62, Q104, S138). Meanwhile, the ferrihydrite nucleation center of HaFerH (D54, H57, E61), HaFerM (E54, E57, E61), and HaFerL (A54, Q57, E61) occupied different residues (Table 2). Unlike some arthropod and mollusk ferritins, vertebrate ferritins typically contain no signal peptides [28,34]. Accordingly, HaFer subunits possessed no signal peptides, suggesting that they all are cytosolic proteins.

In mammals, the FerH subunit is equipped with a conserved ferroxidase diiron center and converts iron (II) to iron (III) in the presence of molecular oxygen [35]. The FerL subunit of mammals lacks such a center; however, it possesses a nucleation center furnished with three glutamic acids facing toward the center of the apoferritin shell, which nucleate and facilitate iron accumulation [36]. Consequently, the FerH and FerL subunits have distinct and complementary functions.

To examine the conservation of HaFer in the context of its mammalian and fish homologs, multiple sequence alignments were generated using sequences of three ferritin subunit types. The results illustrated a higher degree of conservation in iron binding region signatures and iron binding sites (Fig. 2). The residues in the ferroxidase diiron center of HaFerH were completely conserved with respect to other FerH homologs [21], suggesting its potential capacity to oxidize iron (II) [35]. Of the three conserved glutamic acids in the ferrihydrite nucleation center, the second residue varies in fish FerLs [18]. Unlike other homologs, the first glutamic acid was also replaced by A54 in HaFerL, which might possibly influence its role in nucleation. It was interesting to note that HaFerM exhibited ideal conservation with respect to both the ferroxidase diiron center of mammalian FerH, and the ferrihydrite micelle nucleation center of mammalian FerL, evidencing its dual capacity to perform the iron oxidation and iron mineralization functions efficiently.

While the tight conservation of ferritins was evidenced from the multiple alignments, the pairwise homology between HaFers and their corresponding teleost homologs was high. Comparatively, FerH and FerM members share a strong identity (75–97%), whereas FerL members shared a quite low identity (45–78%). Taken together, these *in silico* data support the conclusion that the three sequences isolated in this study are true orthologs of the FerH, FerM, and FerL subunits. Unlike mammals, which possess only FerH and FerL, teleosts can be added to the lower order vertebrate category that expresses all three ferritin subunits as shown in bullfrogs [23]. It appears therefore that fish ferritins could be assembled either as heteropolymers consisting of FerH and FerL subunits, or as homopolymers composed of FerM subunits.

3.2. Phylogenetic analysis of vertebrate ferritin subunits

A phylogenetic tree was constructed by the NJ method using amino acid sequences of three ferritin subunits from different animal origins. As illustrated in Fig. 3, the resultant tree revealed a clear clustering of sequences based on subunit types including ferritin H, M, and L. The respective fish and mammalian ferritin subunits clustered closely and independently in each main branch, where HaFerH, HaFerM, and HaFerL are associated with fish ferritins with significant bootstrap support substantiating their homology with their respective teleost counterparts. FerM subunit members exhibited exclusively a piscine origin, clearly showing

Table 2
Comparison of molecular profiles of *H. abdominalis* ferritin subunits.

	Characteristics	HaFerH	HaFerM	HaFerL
Nucleotide (cDNA)	GenBank accession No	KP780174	KP780175	KP780176
	ORF (bp)	534	531	525
	5′-UTR	607	180	91
	3′-UTR	479	36	223
	IRE in 5′-UTR	TTACCTGCTTCAACAGTGCTTGAACGGCAAC	GTTCTTGCTTCAACAGTGATTGAACGGAACT	Not present
	Polyadenylation signal/poly A tail	AATAAA; present	Not determined	AATAAA; present
Protein	Peptide (aa)	177	176	174
	Molecular mass (Da)	21	21	20
	Theoretical *p*I	5.44	5.36	5.77
	Ferritin-like diiron domain profile	7–156	7–156	7–156
	IBRS	2 (58–76 and 123–143)	1 (123–143)	1 (123–143)
	Residues at ferroxidase center	E24, Y31, E58, E59, H62, E104, Q138	E24, Y31, E58, E59, H62, E104, Q138	Not fully conserved
	Residues at nucleation center	Not fully conserved	E54, E57, E61	A54, Q57, E61
	Highest homology	*O. fasciatus* FerH	*S. ocellatus* FerM	*A. fimbria* FerL
	Signal peptide/location	No; cytoplasm	No; cytoplasm	No; cytoplasm
Transcripts	Highest mRNA level (qPCR)	PBCs	Liver	PBCs
Protein activity	Ferroxidase activity	Present; strong even at lower dose	Present; strong even at lower dose	Present; only at higher dose

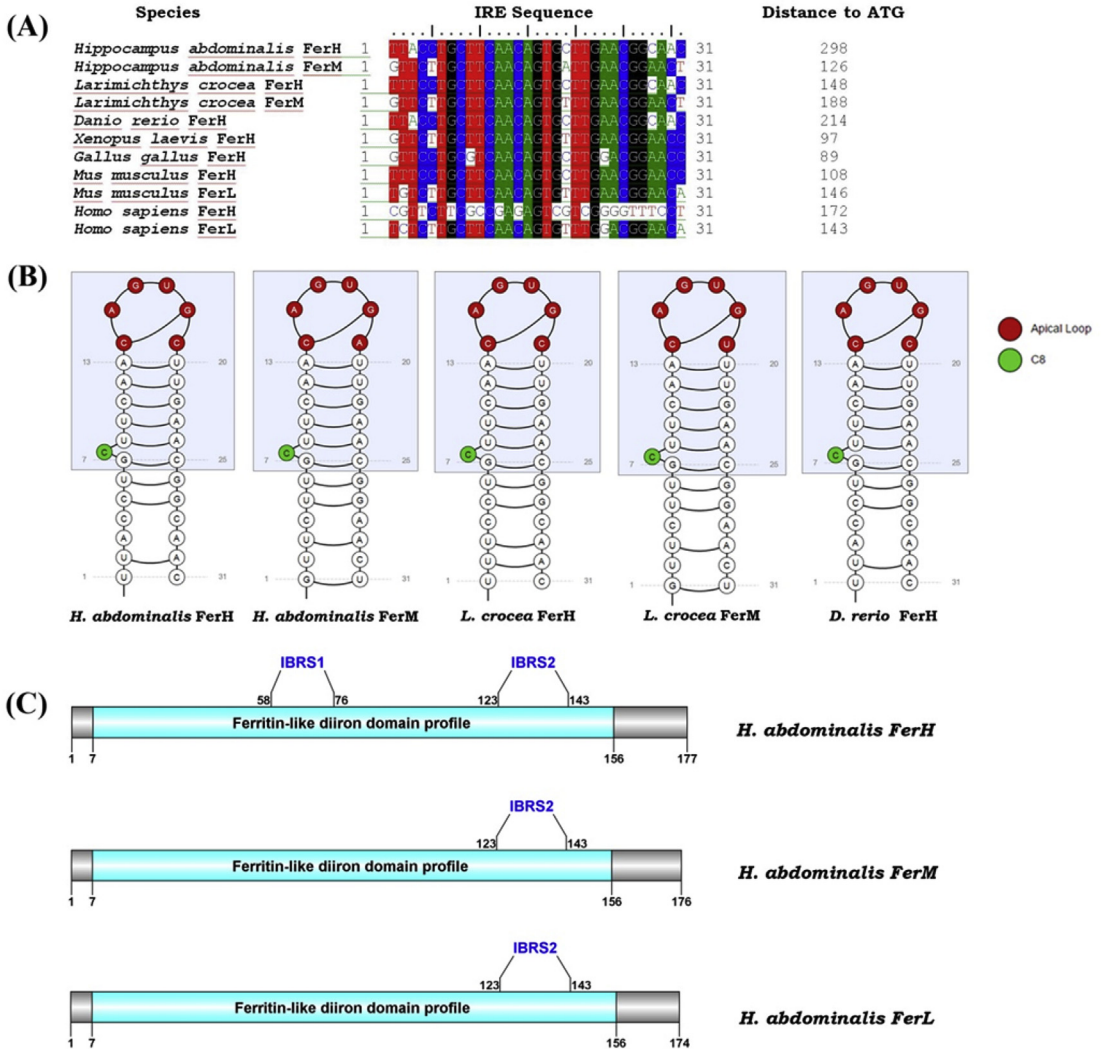

Fig. 1. Characteristics of iron responsive elements (IREs) in the 5′-UTR of *H. abdominalis* ferritin subunit mRNAs, and the domain organization of translated products. (A) Sequence alignment of IREs from selected vertebrate ferritins. The distance of the IREs from the start codons is given in bp. (B) Predicted stem-loop structures of IREs from selected fish species. Apical loop and bulging Cys (C8) are shown in colors. (C) Domain composition of seahorse ferritins. Locations of iron-binding region signatures (IBRSs) are shown. (For interpretation of the references to color in this figure legend, the reader is referred to the web version of this article.)

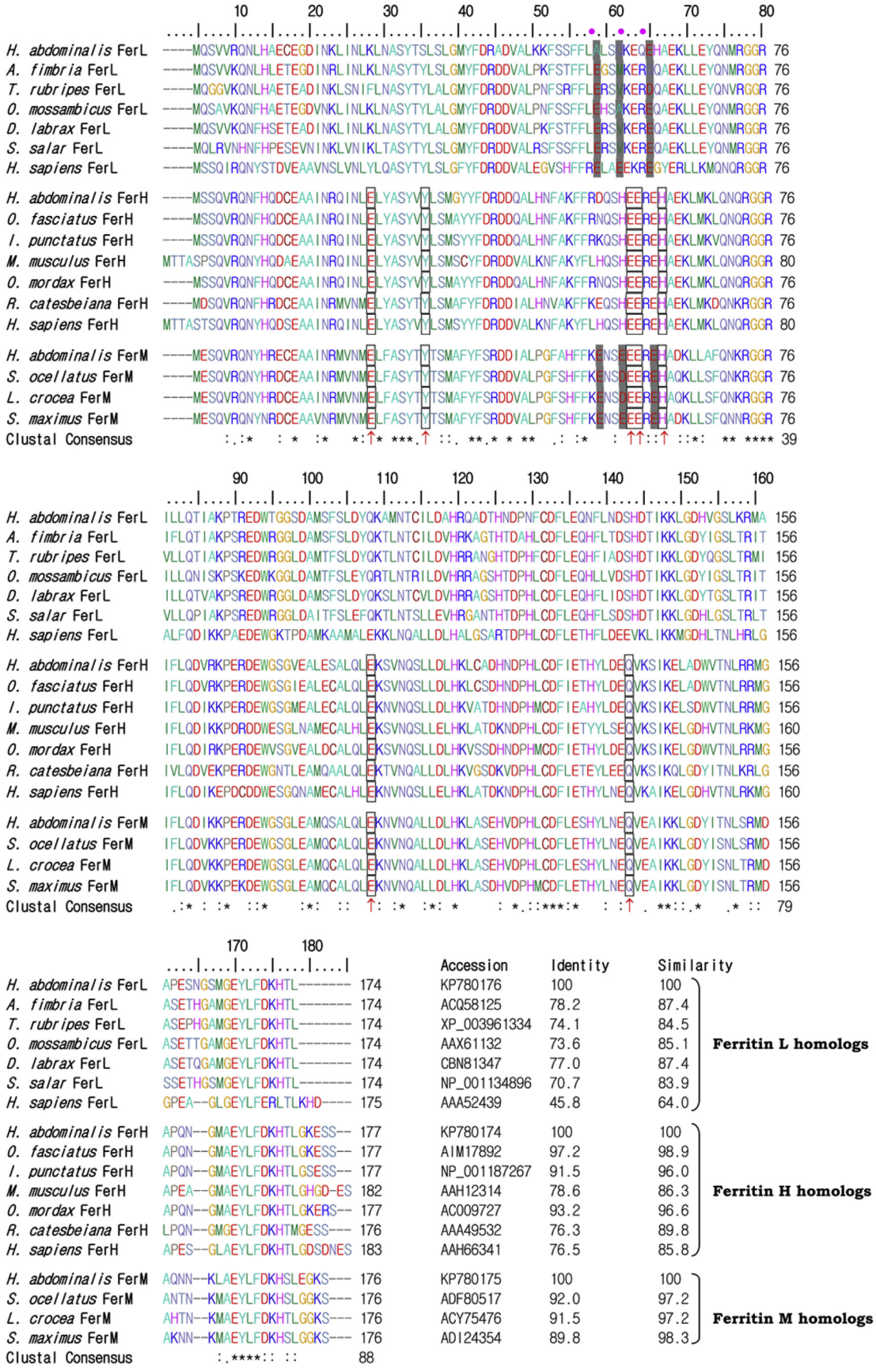

Fig. 2. Multiple sequence alignment of different vertebrate ferritin subunits and homology scores of *H. abdominalis* ferritin subunits with their corresponding counterparts. Sequence alignments were performed using the ClustalW method. The amino acids are numbered along the right margin. Identical residues in all sequences are indicated by asterisks (*) under the columns. Residues strongly and weakly conserved are indicated by colons (:) and dots (.), respectively. Seven conserved amino acids composing the ferroxidase center (of H and M subunits) are indicated with red arrows. Residues involved in iron nucleation (in L and M subunits) are indicated by purple dots. Identity and similarity scores of each HaFer sequence with its respective homolog are indicated at the end of the sequence.

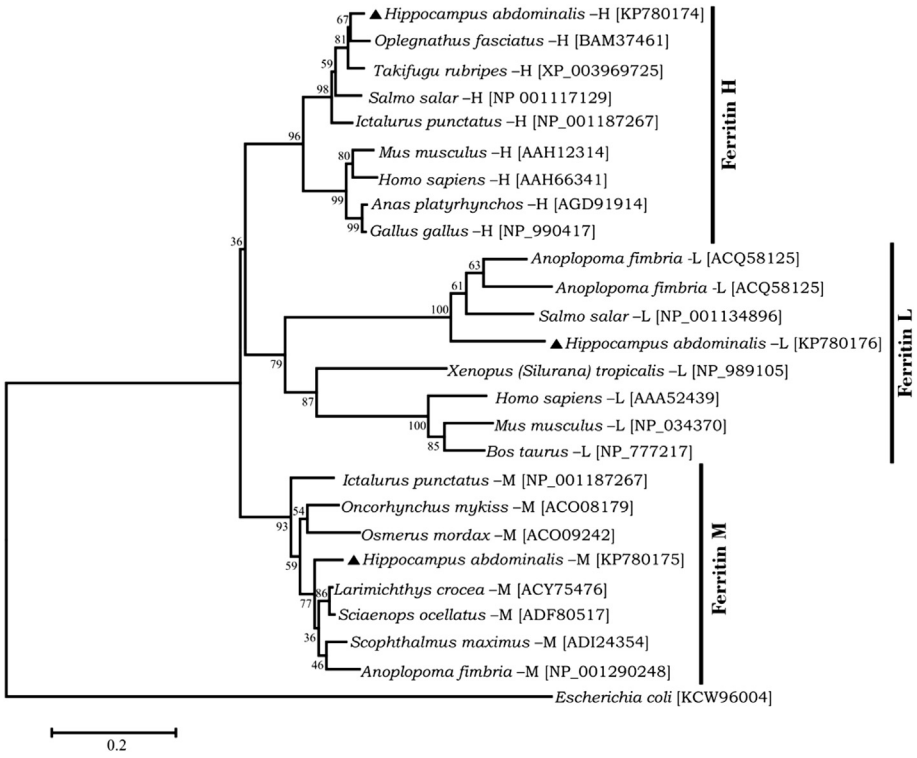

Fig. 3. Phylogenetic relationships of *H. abdominalis* ferritin subunits and their known orthologs. Evolutionary proximity of different seahorse ferritin subunits and their vertebrate counterparts was analyzed on the basis of ClustalW alignments of the respective protein sequences by using the NJ method in MEGA 5.0 software. Corresponding bootstrap values are indicated on the branches.

their limited distribution among lower order vertebrates in the animal kingdom [23], and they formed the basal branch from which the other two branches evolved (Fig. 3).

There are controversial views about the evolution of ferritin subunits. One hypothesis suggested that FerH is the common ancestor, from which FerM evolved initially, followed by FerL [16]. Scudiero et al. (2013) proposed an alternative view, that a FerM-like form was the ancestral form of other ferritin subunits [37]. Unlike those studies, our analysis included the FerL sequence(s) of fish origin, and the topology of our phylogenetic dendrogram implies that FerM could be the potential ancestor of FerH and FerL. Based on our results, we believe that FerH and FerL, which have distinct and complementary roles (oxidation and mineralization of iron), could have evolved from a FerM ancestor possessing those dual functions. Subsequently, FerM could have disappeared during the evolution of higher order vertebrates. However, detailed evolutionary analyses are required to validate this opinion regarding ferritin evolution.

Although the transcriptome data mining in this study has identified a single isoform of each ferritin subunit, we cannot exclude the possibility of the existence of multiple ferritin isoforms in seahorses. Evidence suggests that whole genome duplication events in teleosts have led to the existence of multiple ferritin isoforms as reported in salmonids [18,32].

3.3. Purification of recombinant HaFers and assessment of their purity

In order to investigate the biological function of the three *H. abdominalis* ferritin subunits, we cloned them into a pMAL-c2X vector and overexpressed them in an *E. coli* system. Recombinant HaFer (rHaFer) proteins were then purified by an affinity chromatography approach. The eluted rHaFerH, rHaFerM, and rHaFerL fusion proteins were analyzed on a 12% SDS-PAGE and the results indicated that all three rHaFer fusion proteins were resolved to single bands (lane 5 in each gel; Fig. 4). Moreover, all the protein products appeared to harbor corresponding rHaFer subunits along with an MBP-tag complying with their predicted molecular masses (rHaFer: ~20–21 kDa; MBP: 42.5 kDa), resulting in fusion proteins with molecular masses around 62–63 kDa (Fig. 4).

3.4. Iron (II) depriving activity

In order to analyze the iron (II) depriving activity of rHaFer fusion proteins, a chromogenic assay was employed. This assay quantifies the iron (II) binding proteins based on the reduction in absorbance of the Fe^{2+}-ferrozine complex at OD 562 nm. As illustrated in Fig. 5, all three rHaFer fusion proteins demonstrated detectable iron (II) withholding activity. Absorbance values of the final reaction mixtures at 562 nm decreased with the increasing dose (0–80 μg) of each rHaFer subunit, and the control experiment with rMBP did not show any significant iron chelation at any concentration. In general, FerH and FerM demonstrate ferroxidase activity by converting iron (II) ions to iron (III) ions [6]. Both rHaFerH and rHaFerM significantly chelated iron (II) at a 20 μg dose level, as reflected by the plot in Fig. 5. The presence of essential residues at the ferroxidase center of HaFerH and HaFerM, as per our *in silico* prediction, supports the above observed biological activity. Intriguingly, we were able to detect significant iron (II) depriving activity for rHaFerL at higher doses (>40 μg). It has been clearly shown that residues at the ferroxidase center are the determinants of ferroxidase activity, and using site-directed mutagenesis such a center was constructed in a human FerL chain with a different combination of residues, and it displayed ferroxidase activity [38]. The observed ferroxidase activity of rHaFerL might be at least in part because of the presence of partially conserved residues typical of ferroxidase centers, including E59 and H62 in the HaFerL protein (Fig. 2). Formation of reactive oxygen species (ROS) could be facilitated by excess iron that has detrimental effects on protein, lipid,

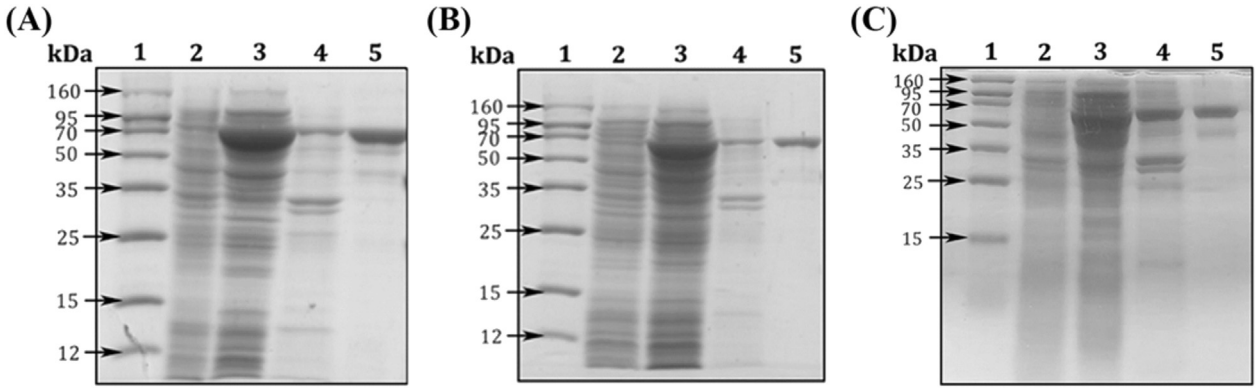

Fig. 4. SDS-PAGE analysis of inductively overexpressed and purified recombinant ferritin subunits of *H. abdominalis*; (A) rHaFerH, (B) rHaFerM, (C) rHaFerL fusion proteins. Lane 1, protein marker (Enzynomics, Korea); 2, total cellular extract from *E. coli* BL21 (DE3) prior to IPTG-induction; 3, whole cell lysate after IPTG-induction (1 mM) at 37 °C for 3 h; 4, crude extract of rHaFer proteins from lysate (#3); 5, purified rHaFer fusion proteins from lane 4 by affinity chromatography.

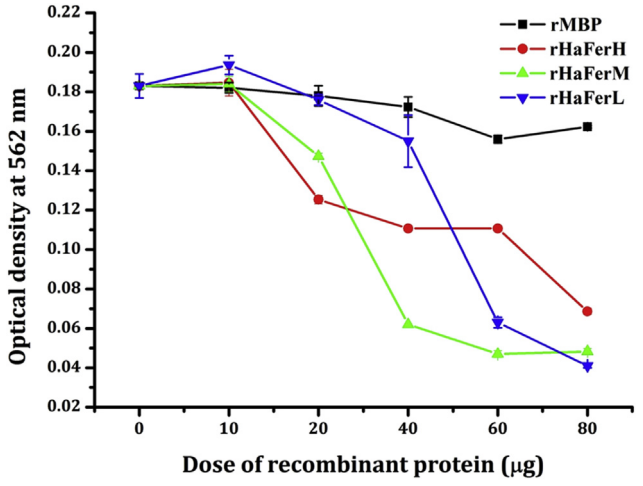

Fig. 5. *In vitro* iron withholding assay for recombinant ferritin subunits of *H. abdominalis*. $FeSO_4$ was incubated with increasing amounts of rHaFer subunit proteins (0–80 μg). Following the addition of ferrozine, OD_{562} was measured. Error bars represent the SD (n = 3).

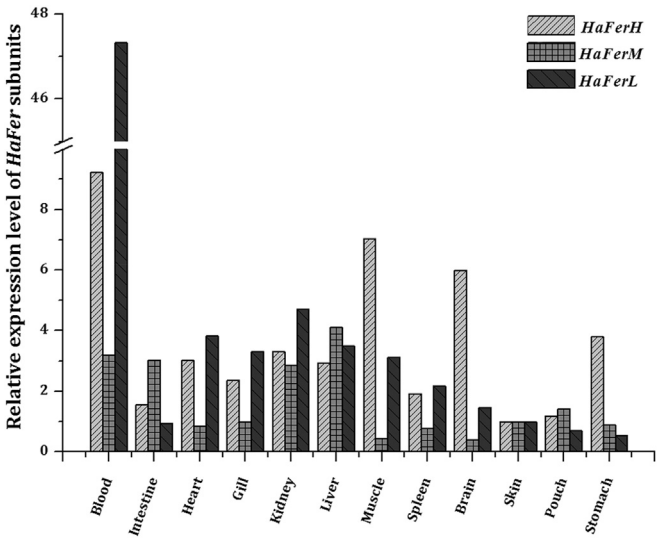

Fig. 6. The transcriptional distribution of *H. abdominalis* ferritin subunits as determined by qPCR. Relative expression was calculated by the $2^{-\Delta\Delta Ct}$ method using the seahorse 40S ribosomal protein S7 as the internal reference gene. Fold changes in expression are shown relative to the mRNA expression level in the skin for three replicate real–time reactions from pooled tissue of six individual seahorses.

and DNA. Their ability to sequester iron (II), as evidenced from our study, makes HaFers vital elements in systemic iron homeostasis.

3.5. Expression of ferritin subunits in tissues of healthy *H. abdominalis*

HaFer expression profiles (Fig. 6) revealed that mRNAs of all three *HaFer* subunits were widely distributed in the tissues examined. The relative mRNA expression fold of each *HaFer* subunit was calculated using the *H. abdominalis* 40S ribosomal protein S7 as the internal reference gene, further normalizing the expression of each tissue to that of the skin. The *HaFerH* and *HaFerL* mRNA expression levels were highest in PBCs. As reported previously, *FerH* subunits of two Antarctic notothenioids, catfish, rock bream, red drum, and sea bass were predominantly expressed in the liver and/or blood [16,19,22,39,40]. Meanwhile, two isoforms of *FerH* in *S. salar* (H1 and H2) were detected at high levels in the muscle [18], agreeing with our observations. On the other hand, the expression level of *HaFerM* was highest in the liver followed by PBCs when compared to other tissues. The *FerM* mRNA of *C. semilaevis* and large yellow croaker was abundantly found in the liver, and its *O. fasciatus* counterpart was highly expressed in PBCs [6,20,21]. While *HaFerM* expression was in accordance with these profiles, the expression pattern of three *FerM* isoforms (M1–M3) in *S. salar* varied markedly in a tissue specific manner [18], and another variant had distinctive transcription levels in gonad [5]. Ferritin mRNA distribution in mammals is markedly different from that in fish. Mammalian *FerH* subunits are abundant in the heart and brain, where they potentially, through their rapid iron (II) depriving activity, are involved in iron detoxification. On the other hand, mammalian *FerL* subunits are abundantly found in the liver, where they act as iron reservoirs [41]. Our data clearly revealed that *HaFerL* might be a PBC-specific ferritin based on its relative fold in tissues. The pronounced expression of *HaFer* subunits in blood is very likely to be observed since some blood cells, including macrophages, store iron after erythrophagocytosis and then generally release it under the regulation of iron regulatory proteins such as ferritins [42,43]. On the other hand, it can also be attributed to the iron-withholding properties of ferritins, which impart to hosts an anti-microbial defense in blood enriched with immune cells [14]. The liver is a well-known center of iron storage and metabolism in animals

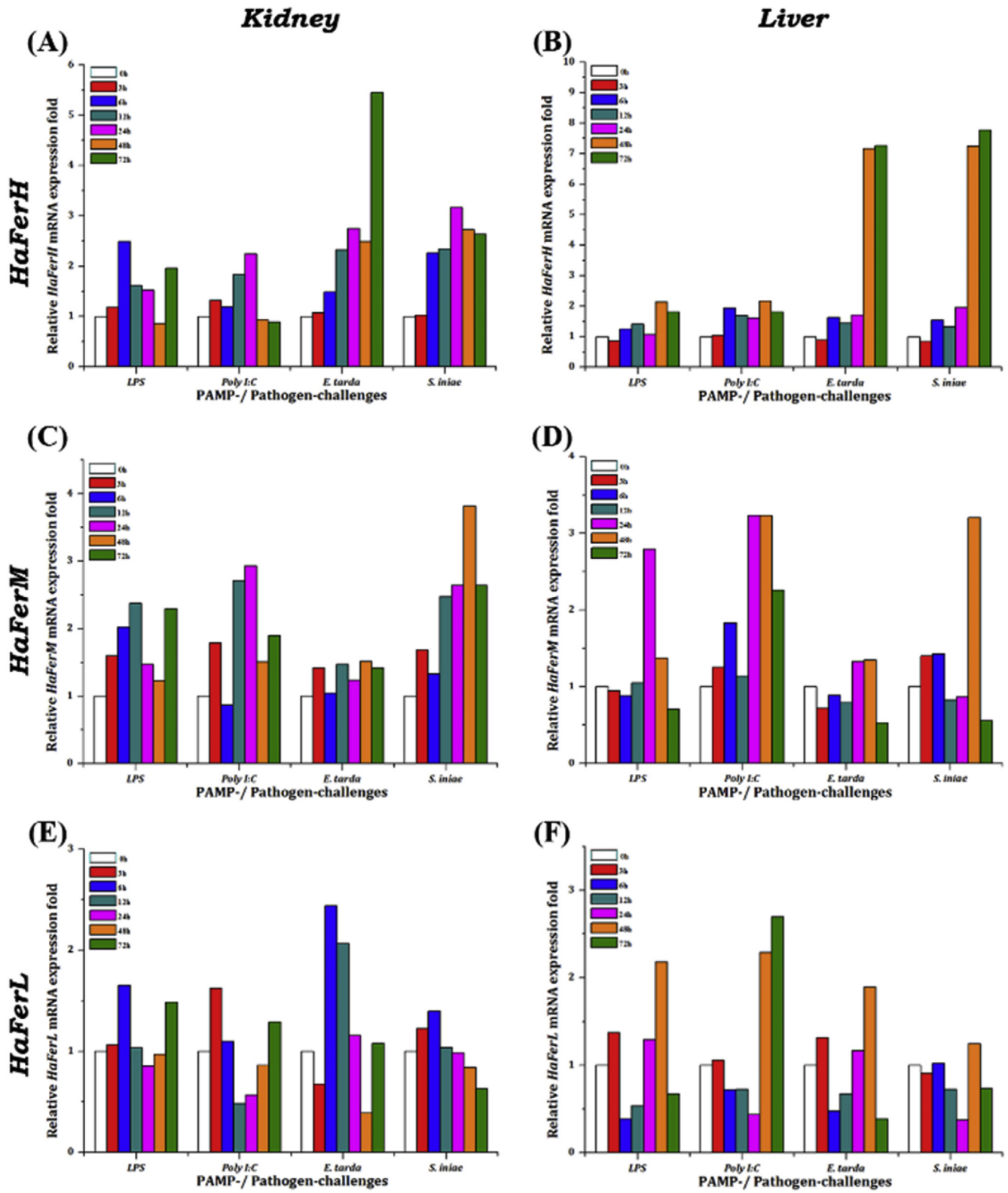

Fig. 7. Immune responsive expression profiles of *H. abdominalis* ferritin subunits in the kidney (A, C, E) and liver (B, D, F) upon different immune challenges as determined by qPCR. Relative expression was calculated by the $2^{-\Delta\Delta Ct}$ method using the seahorse 40S ribosomal protein S7 as the reference gene with respect to the corresponding PBS-injected controls at each time point. The relative fold change in expression at 0 h post-injection was used as the basal line for three replicate real–time reactions from pooled tissue of five individual seahorses.

[44,45]. Moreover, it harbors significant numbers of immune cells and acts as an immune organ to combat pathogenic infections [46], probably mediated by iron deprivation in cells as one of the defense strategies. Thus, we would expect a higher level of basal ferritin expression in the liver tissue. Basal expression of *HaFer*s in naïve seahorse suggests that they may play important tissue-specific

roles.

3.6. Modulation of mRNA expression under pathogen-stress

In order to investigate the host immune response in terms of ferritin subunit expression, subunit mRNA levels were determined in kidney and liver tissues by qPCR, after stimulating healthy seahorses with different pathogens and associated molecular patterns. Based on our qPCR data, three *HaFer* subunits were found to modulate their basal expression in a tissue-specific manner. Herein, we have used LPS (an endotoxin in the cell walls of Gram-negative bacteria), and poly I:C (a viral double stranded RNA mimic) as pathogen-derived mitogens, along with common aquatic microbes including *E. tarda* and *S. iniae* as live bacterial pathogens (Fig. 7). The dose and volume of LPS used in this study appeared to be higher, when compared with previous studies [47,48]. However, there were no acutely toxic effects observed during the whole challenge experiment. Further, no behavioral changes or mortality were observed during this period. Nevertheless, additional studies are required to conduct in order to examine the toxic effect LPS on seahorse.

Transcriptional expression of *HaFerH* was induced by all the devised challenges in both kidney and liver, where at least a ~2-fold increase was noticed at the time point of highest induction against each injection (Fig. 7A, B). Notably, the fold increase in *HaFerH* mRNAs caused by experimental infection with live bacteria (>7-fold in the liver and >2.5-fold in the kidney) was higher than in those with PAMPs in both tissues. Fig. 7C and D illustrate the post-injection time course modulation of *HaFerM* expression. *E. tarda* infection had no effect on its mRNA expression in the kidney, and a moderate impact in liver (1.35-fold). However, *S. iniae* infection evoked an inductive transcriptional response in the kidney and liver with 3.2- and 3.8-fold increases, respectively. Both PAMPs elicited significantly elevated mRNA levels in the kidney and liver, where poly I:C-induced *HaFerM* expression was marginally higher than that of LPS. Deviating from the expression patterns of *HaFerH* and *HaFerM* against pathogen-induced stress, *HaFerL* transcription differed over time in response to immune challenges (Fig. 7E, F). The mRNA level of *HaFerL* fluctuated considerably throughout the period of injection trials with significant up- and down-regulation. *E. tarda* (2.7-fold) and poly I:C (2.4-fold), respectively, led to a strong response in the kidney and liver.

In mammals, evidence exist for modulation of ferritin synthesis mediated by inflammatory conditions such as microbial infections [2,49]. Similarly, several research groups have reported upregulated expression of *FerH* and *FerM* subunits in fish species under pathological conditions. Isoforms of Atlantic salmon ferritin H and M differentially responded against attenuated *Aeromonas salmonicida* infection [18]. Likewise, ferritin H [19] and M [6] subunits in rock bream and large yellow croaker [21] were shown to be induced by bacteria (and virus). Red drum and turbot responded to bacterial infection(s) by increasing the basal expression of *FerM* subunits [10,22]. The overall transcriptional modulation of the three ferritin subunits observed in the current study, together with previous findings, suggests that sensing the molecular patterns of pathogens led the signaling mechanisms to trigger ferritin synthesis. Based on fold changes in *HaFer* transcripts, we suggest that *HaFerH* and *HaFerM* may potentially form ferritin complexes rich in H- and M-chains, which are prominently involved in iron (II) withholding functions [14]. The H and M subunits of these ferritin complexes suppress pathogen growth in cells more effectively than L subunits, which are mainly responsible for the nucleation process [4]. On the other hand, these positive transcriptional responses might represent a temporal elevation of ROS in response to pathogen invasion, which could be possibly counterbalanced by ferritins through their iron (II) depriving activity [9]. The inductive transcriptional responses in the kidney were continuous throughout the experiment, particularly for *HaFerH* and *HaFerM*, when compared to those in the liver. This might be at least in part because of different mechanisms engaged by the liver and kidney tissues to combat invading organisms. On the other hand, as a potent immune organ [50] that is metabolically highly active, the liver may act against pathogen infections by maintaining a high level of ROS in hepatic cells while dynamically regulating local ferritin expression, which can in turn inhibit the Fenton type reactions by depriving free iron (II) ions [51]. Infection-mediated transcriptional upregulation of *HaFer*s in the liver further suggest that they are potent molecules that take part in acute phase responses [52].

Unlike mammals, which have ferritins made up of H and L chains with distinct functional specificity, the lower order vertebrates possess three types of ferritin chains (H, L, and M). It is therefore likely that teleosts are capable of having dynamic control over iron homeostasis, due to the existence of three types of ferritin chains.

4. Conclusion

Our evidence provides an overall insight into the three seahorse ferritins (HaFers: H, M, and L) that structurally resemble the known ferritins and that demonstrate detectable iron (II) chelation activity together with distinct expression profiles. Predictably, these proteins possess conserved structural elements, which are necessary for their biological properties. Evolutionarily, the ferritin M chain seems to precede the other two chains (H and L). The iron depriving activity of the three recombinantly expressed subunits suggests a possible role of HaFers in iron homeostasis. In addition, the three *HaFer*s appeared to be transcriptionally up-regulated from their basal levels under the stress triggered by pathogen-derived mitogens or live pathogens, suggesting that they play a role in host immune defense. Collectively, these findings indicate that the ferritin subunits identified from seahorse are potential role players in iron homeostasis and putatively in host antimicrobial defense, probably by inhibiting pathogen growth through iron (II) deprivation.

Acknowledgments

This research was a part of the project titled 'Fish Vaccine Research Center', and a part of the project titled 'A study on the commercialization of seahorses' funded by the Ministry of Oceans and Fisheries, Korea.

Appendix A. Supplementary data

Supplementary data related to this article can be found at http://dx.doi.org/10.1016/j.fsi.2015.12.039.

References

[1] P.M. Harrison, P. Arosio, The ferritins: molecular properties, iron storage function and cellular regulation, Biochimica Biophysica Acta BBA Bioenerg. 1275 (1996) 161–203.
[2] K. Orino, K. Watanabe, Molecular, physiological and clinical aspects of the iron storage protein ferritin, Vet. J. 178 (2008) 191–201.
[3] G.A. Clegg, J.E. Fitton, P.M. Harrison, A. Treffry, Ferritin: molecular structure and iron-storage mechanisms, Prog. Biophy. Mol. Biol. 36 (1980) 56–86.
[4] S. Levi, P. Santambrogio, A. Cozzi, E. Rovida, B. Corsi, E. Tamborini, et al., The role of the L-chain in ferritin iron incorporation: studies of homo and heteropolymers, J. Mol. Biol. 238 (1994) 649–654.
[5] O. Andersen, A. Dehli, H. Standal, T. Giskegjerde, R. Karstensen, K. Rørvik, Two ferritin subunits of Atlantic salmon (Salmo salar): cloning of the liver cDNAs and antibody preparation, Mol. Mar. Biol. Biotechnol. 4 (1995) 164–170.
[6] D.A. Elvitigala, H.K. Premachandra, I. Whang, M.J. Oh, S.J. Jung, C.J. Park, et al.,

A teleostean counterpart of ferritin M subunit from rock bream (Oplegnathus fasciatus): an active constituent in iron chelation and DNA protection against oxidative damage, with a modulated expression upon pathogen stress, Fish. Shellfish Immunol. 35 (2013) 1455–1465.
[7] F.M. Torti, S.V. Torti, Regulation of ferritin genes and protein, Blood 99 (2002) 3505–3516.
[8] A.M. Thomson, J.T. Rogers, P.J. Leedman, Iron-regulatory proteins, iron-responsive elements and ferritin mRNA translation, Int. J. Biochem. Cell Biol. 31 (1999) 1139–1152.
[9] R.R. Crichton, S. Wilmet, R. Legssyer, R.J. Ward, Molecular and cellular mechanisms of iron homeostasis and toxicity in mammalian cells, J. Inorg. Biochem. 91 (2002) 9–18.
[10] W-j Zheng, Y-h Hu, L. Sun, Identification and analysis of a Scophthalmus maximus ferritin that is regulated at transcription level by oxidative stress and bacterial infection, Comp. Biochem. Physiol. Part B Biochem. Mol. Biol. 156 (2010) 222–228.
[11] K. Salinas-Clarot, A.P. Gutiérrez, G. Núñez-Acuña, C. Gallardo-Escárate, Molecular characterization and gene expression of ferritin in red abalone (Haliotis rufescens), Fish shellfish Immunol. 30 (2011) 430–433.
[12] N. Aziz, H.N. Munro, Iron regulates ferritin mRNA translation through a segment of its 5′untranslated region, Proc. Natl. Acad. Sci. 84 (1987) 8478–8482.
[13] J.V. Neves, J.M. Wilson, P.N. Rodrigues, Transferrin and ferritin response to bacterial infection: the role of the liver and brain in fish, Dev. Comp. Immunol. 33 (2009) 848–857.
[14] S.T. Ong, J.Z.S. Ho, B. Ho, J.L. Ding, Iron-withholding strategy in innate immunity, Immunobiology 211 (2006) 295–314.
[15] S. Recalcati, P. Invernizzi, P. Arosio, G. Cairo, New functions for an iron storage protein: the role of ferritin in immunity and autoimmunity, J. Autoimmun. 30 (2008) 84–89.
[16] H. Liu, T. Takano, E. Peatman, J. Abernathy, S. Wang, Z. Sha, et al., Molecular characterization and gene expression of the channel catfish ferritin H subunit after bacterial infection and iron treatment, J. Exp. Zool. Part A Ecol. Genet. Physiol. 313 (2010) 359–368.
[17] W-j Zheng, Y-h Hu, Z-z Xiao, L. Sun, Cloning and analysis of a ferritin subunit from turbot (*Scophthalmus maximus*), Fish shellfish Immunol. 28 (2010) 829–836.
[18] J.H. Lee, N.J. Pooley, A. Mohd-Adnan, S.A. Martin, Cloning and characterisation of multiple ferritin isoforms in the Atlantic salmon (Salmo salar), PloS One 9 (2014).
[19] D.A.S. Elvitigala, B.-S. Lim, I. Whang, S.-Y. Yeo, C.Y. Choi, J. Lee, Molecular profile and functional characterization of the ferritin H subunit from rock bream (*Oplegnathus fasciatus*), revealing its putative role in host antioxidant and immune defense, Dev. Comp. Immunol. (2014).
[20] W. Wang, M. Zhang, L. Sun, Ferritin M of *Cynoglossus semilaevis*: an iron-binding protein and a broad-spectrum antimicrobial that depends on the integrity of the ferroxidase center and nucleation center for biological activity, Fish Shellfish Immunol. 31 (2011) 269–274.
[21] X. Zhang, W. Wei, H. Wu, H. Xu, K. Chang, Y. Zhang, Gene cloning and characterization of ferritin H and M subunits from large yellow croaker (*Pseudosciaena crocea*), Fish Shellfish Immunol. 28 (2010) 735–742.
[22] Y-h Hu, W-j Zheng, L. Sun, Identification and molecular analysis of a ferritin subunit from red drum (*Sciaenops ocellatus*), Fish Shellfish Immunol. 28 (2010) 678–686.
[23] L.F. Dickey, S. Sreedharan, E.C. Theil, J.R. Didsbury, Y.H. Wang, R.E. Kaufman, Differences in the regulation of messenger RNA for housekeeping and specialized-cell ferritin. A comparison of three distinct ferritin complementary DNAs, the corresponding subunits, and identification of the first processed in amphibia, J. Biol. Chem. 262 (1987) 7901–7907.
[24] J.L. Balcázar, A. Gallo-Bueno, M. Planas, J. Pintado, Isolation of Vibrio alginolyticus and Vibrio splendidus from captive-bred seahorses with disease symptoms, Antonie Leeuwenhoek 97 (2010) 207–210.
[25] A.C. Vincent, R.S. Clifton-Hadley, Parasitic infection of the seahorse (Hippocampus erectus)-a case report, J. Wildl. Dis. 25 (1989) 404–406.
[26] K. Tamura, J. Dudley, M. Nei, S. Kumar, MEGA4: molecular evolutionary genetics analysis (MEGA) software version 4.0, Mol. Biol. Evol. 24 (2007) 1596–1599.
[27] M.M. Bradford, A rapid and sensitive method for the quantitation of microgram quantities of protein utilizing the principle of protein-dye binding, Anal. Biochem. 72 (1976) 248–254.
[28] M. De Zoysa, J. Lee, Two ferritin subunits from disk abalone (Haliotis discus discus): cloning, characterization and expression analysis, Fish Shellfish Immunol. 23 (2007) 624–635.
[29] K.J. Livak, T.D. Schmittgen, Analysis of relative gene expression data using real-time quantitative PCR and the 2< sup>− ΔΔCT method, Methods 25 (2001) 402–408.
[30] W. Wang, M. Zhang, L. Sun, Ferritin M of Cynoglossus semilaevis: an iron-binding protein and a broad-spectrum antimicrobial that depends on the integrity of the ferroxidase center and nucleation center for biological activity, Fish Shellfish Immunol. 31 (2011) 269–274.
[31] W.J. Zheng, Y.H. Hu, Z.Z. Xiao, L. Sun, Cloning and analysis of a ferritin subunit from turbot (Scophthalmus maximus), Fish. Shellfish Immunol. 28 (2010) 829–836.
[32] M. Yamashita, N. Ojima, T. Sakamoto, Molecular cloning and cold-inducible gene expression of ferritin H subunit isoforms in rainbow trout cells, J. Biol. Chem. 271 (1996) 26908–26913.
[33] P. Piccinelli, T. Samuelsson, Evolution of the iron-responsive element, RNA 13 (2007) 952–966.
[34] H. Nichol, M. Locke, Secreted ferritin subunits are of two kinds in insects molecular cloning of cDNAs encoding two major subunits of secreted ferritin from Calpodes ethlius, Insect Biochem. Mol. Biol. 29 (1999) 999–1013.
[35] D.M. Lawson, A. Treffry, P.J. Artymiuk, P.M. Harrison, S.J. Yewdall, A. Luzzago, et al., Identification of the ferroxidase centre in ferritin, FEBS Lett. 254 (1989) 207–210.
[36] P. Santambrogio, S. Levi, A. Cozzi, B. Corsi, P. Arosio, Evidence that the specificity of iron incorporation into homopolymers of human ferritin L- and H-chains is conferred by the nucleation and ferroxidase centres, Biochem. J. 314 (1996) 139–144.
[37] R. Scudiero, M.G. Esposito, F. Trinchella, Middle ferritin genes from the icefish Chionodraco rastrospinosus: Comparative analysis and evolution of fish ferritins, Comptes Rendus Biol. 336 (2013) 134–141.
[38] S. Levi, B. Corsi, E. Rovida, A. Cozzi, P. Santambrogio, A. Albertini, et al., Construction of a ferroxidase center in human ferritin L-chain, J. Biol. Chem. 269 (1994) 30334–30339.
[39] R. Scudiero, F. Trinchella, M. Riggio, E. Parisi, Structure and expression of genes involved in transport and storage of iron in red-blooded and hemoglobin-less antarctic notothenioids, Gene 397 (2007) 1–11.
[40] J.V. Neves, J.M. Wilson, P.N.S. Rodrigues, Transferrin and ferritin response to bacterial infection: the role of the liver and brain in fish, Dev. Comp. Immunol. 33 (2009) 848–857.
[41] P.M. Harrison, P. Arosio, The ferritins: molecular properties, iron storage function and cellular regulation, Biochim. Biophys. Acta 31 (1996) 161–203.
[42] M.D. Knutson, M. Oukka, L.M. Koss, F. Aydemir, M. Wessling-Resnick, Iron release from macrophages after erythrophagocytosis is up-regulated by ferroportin 1 overexpression and down-regulated by hepcidin, Proc. Natl. Acad. Sci. U. S. A. 102 (2005) 1324–1328.
[43] K. Hausmann, U. Wulfhekel, J. Düllmann, R. Kuse, Iron storage in macrophages and endothelial cells. Histochemistry, ultrastructure, and clinical significance, Blut 32 (1976) 289–295.
[44] G.J. Anderson, D.M. Frazer, Hepatic iron metabolism, Semin. Liver Dis. (2005) 420–432.
[45] R.M. Graham, A.C. Chua, C.E. Herbison, J.K. Olynyk, D. Trinder, Liver iron transport, World J. Gastroenterol. 13 (2007) 4725.
[46] S. Seki, Y. Habu, T. Kawamura, K. Takeda, H. Dobashi, T. Ohkawa, et al., The liver as a crucial organ in the first line of host defense: the roles of Kupffer cells, natural killer (NK) cells and NK1. 1 Ag+ T cells in T helper 1 immune responses, Immunol. Rev. 174 (2000) 35–46.
[47] P. Balm, E. Van Lieshout, J. Lokate, S.W. Bonga, Bacterial lipopolysaccharide (LPS) and interleukin 1 (IL-1) exert multiple physiological effects in the tilapia Oreochromis mossambicus (Teleostei), J. Comp. Physiol. B 165 (1995) 85–92.
[48] A. Haukenes, B. Barton, Characterization of the cortisol response following an acute challenge with lipopolysaccharide in yellow perch and the influence of rearing density, J. Fish Biol. 64 (2004) 851–862.
[49] M.A. Knovich, J.A. Storey, L.G. Coffman, S.V. Torti, F.M. Torti, Ferritin for the clinician, Blood Rev. 23 (2009) 95–104.
[50] S. Seki, H. Nakashima, M. Kinoshita, The liver as a pivotal innate immune organ, Immunol. Gastroenterol. 1 (2012) 76–89.
[51] C.C. Winterbourn, Toxicity of iron and hydrogen peroxide: the Fenton reaction, Toxicol. Lett. 82 (1995) 969–974.
[52] A.M. Konijn, C. Hershko, Ferritin synthesis in inflammation. I. Pathogenesis of impaired iron release, Br. J. Haematol. 37 (1977) 7–16.